Endogenous Separations and Non-monotone Beveridge Curve Shifts[†]

Hanbaek Lee *University of Cambridge*
Philip Schnattinger *Bank of England*
Francesco Zanetti *University of Oxford*

January 31, 2026

(click here for the latest version)

Abstract

We examine nonlinear Beveridge curve dynamics using a globally solved Diamond-Mortensen-Pissarides model with endogenous job destruction. We theoretically establish that the Beveridge curve shifts outward when matching efficiency increases if and only if the elasticity of job separation with respect to matching efficiency exceeds the match survival rate. This condition arises because higher matching efficiency raises firms' reservation productivity, triggering *churn* that outweighs the direct effect of faster hiring. U.S. data confirm this mechanism, particularly during the post-COVID recovery. We establish that churning-driven unemployment is inefficiently volatile and show that a corporate tax of approximately 5% optimally mitigates this distortion.

Keywords: State-dependence, Nonlinear Labor Market Dynamics, Beveridge curve, unemployment, Business Cycles.

JEL codes: E24, E32, J64

[†] The authors thank Regis Barnichon and Pawel Krolikowski for helpful comments and discussions. All errors are our own. Any views expressed here are solely those of the authors and do not represent those of the Bank of England or any of its committees.
Lee: hl610@cam.ac.uk. Schnattinger: Philip.Schnattinger@gmail.com.
Zanetti: francesco.zanetti@economics.ox.ac.uk

1 Introduction

The Beveridge curve—the inverse relationship between unemployment and job vacancies—is a cornerstone of macro-labor analysis. Standard search theory offers a clear prediction regarding its movements: improvements in matching efficiency should unequivocally lower unemployment for a given level of vacancies, shifting the curve inward. Yet, recent data challenges this fundamental intuition. During the recovery from the COVID-19 pandemic, the U.S. labor market exhibited a puzzling dynamic: matching efficiency was high, yet the Beveridge curve shifted sharply outward. This *efficiency paradox* suggests that the forces driving labor market turnover are more complex than the canonical framework implies.

Standard macroeconomic models with exogenous job separation cannot explain this phenomenon. In these frameworks, higher matching efficiency increases the job-finding rate without affecting the separation rate, necessarily improving the unemployment-vacancy trade-off. To reconcile the model with the data, one would have to assume massive, unobserved negative shocks to other structural parameters. This inability to capture the co-movement of efficiency and unemployment inflows highlights a critical missing channel: the decision to dissolve a match is not independent of the ease of forming a new one.

In this paper, we resolve this puzzle by analyzing the Diamond-Mortensen-Pissarides (DMP) model with endogenous job destruction using a global nonlinear solution. We identify a "churning channel" that overturns standard intuition: when matching efficiency rises, the expected cost of filling a vacancy falls. This lowers the value of retaining a marginal worker, prompting firms to raise their reservation productivity and shed low-quality matches. We demonstrate that when the elasticity of this separation response is sufficiently high, it overwhelms the direct effect of faster hiring, causing the Beveridge curve to shift outward. This mechanism successfully replicates the nonlinear dynamics observed during the COVID-19 recovery—where high efficiency paradoxically triggered a surge in separations—without relying on ad-hoc shocks.

Beyond explaining Beveridge-curve shifts, our framework delivers a disciplined efficiency benchmark. In standard search models, the decentralized equilibrium is constrained efficient only when the Hosios condition holds pointwise. With a non-

constant matching elasticity, a fixed Nash bargaining weight implies that this condition is violated away from the steady state, generating state-dependent inefficiencies in vacancy creation and, in our model, endogenous separations.

We therefore compute a *Hosios-efficient global path* by allowing the bargaining weight to adjust endogenously with tightness so that the Hosios condition holds at each date along the transition. In our calibration, the efficient benchmark has a similar mean unemployment rate to the baseline (around 4.5%) but substantially lower volatility (unemployment s.d. 8.71% vs. 10.58% in the baseline). This "efficiency gap" is largest in high matching-efficiency states, precisely when the churning channel is strongest.

Building on this benchmark, we conduct a historical analysis of unemployment dynamics by replicating two major recessions: COVID-19 and the Great Recession. We show that the outsized outward Beveridge-curve shift during the COVID-19 recovery can be accounted for by high matching efficiency interacting with endogenous job destruction, whereas the Great Recession features persistently low matching efficiency and muted churning dynamics.

Finally, we use the efficient benchmark to evaluate simple fiscal instruments. We show that a modest corporate tax/firing penalty can substantially reduce inefficient churn and bring the baseline transition closer to the efficient path in high-efficiency episodes.

Related literature Our research is most closely related to the series of contributions by Petrosky-Nadeau and Zhang (Petrosky-Nadeau and Zhang, 2017, 2021) studying the non-linear dynamics of the DMP model with exogenous job destruction. We differ from their contributions along three dimensions. We explicitly focus on understanding Beveridge curve shifts in this non-linear framework. Second, we include endogenous job separations. Endogenous job separations is difficult to capture with their projection solution. Instead we employ the sequence-space-based solution method developed in Lee (2025). Third, we include an analysis of optimal policy in this accurately solved model. It is worth noting that earlier work by Fujita and Ramey (2012), has shown that the DMP model with endogenous separation does not produce a stable Beveridge curve relationship. Our globally solved framework, however, demonstrates that this conclusion depends importantly on the solution method employed: even in the absence of matching efficiency fluctuations, the model with

endogenous separation generates a well-defined Beveridge curve, reinforcing the importance of the calibration and accurate nonlinear solution techniques for fitting the Beveridge curve.

Beveridge curve shifts have been at the center of recent debates about the labor market and the labor market effects on inflation (Barnichon and Shapiro, 2024; Crump et al., 2024). Barlevy et al. (2024) argue that there are changing reasons for Beveridge curve shifts. We focus in this paper on shifts induced by the co-movement of matching efficiency and the separations rate increasing. These shifts are particularly interesting as they affect churn in the labor market. The Beveridge curve shifts out during these shifts as the effect of a higher separations rate induced by higher matching efficiency outweighs the inward shifting direct effect of an increase in matching efficiency. Barlevy et al. (2024) argue that this shift was prevalent during the recovery from the pandemic.

We also contribute to the literature on optimal policy in the DMP model, as discussed in Pissarides (2000). While Jung and Kuester (2015) extends this analysis to a dynamic setting, our global non-linear solution provides new insights by accurately computing higher-order moments. This precision allows us to highlight the mean-variance trade-off in firing taxes and examine how policymakers can either minimize unemployment volatility or maximize efficiency with positive firing taxes. These trade-offs arise from the impact of hiring taxes on separation and hiring rates, as well as on worker selection and productivity.

Roadmap The paper is organized as follows. Section 2 presents empirical evidence on the Beveridge curve, focusing on shifts driven by variations in matching efficiency and separation rates. Section 3 develops the model, while Section 4 details our global non-linear solution method and examines its quantitative implications for Beveridge curve shifts, state dependency, and non-linearity. We also assess the model's fit to the data. In Section 5, we introduce inefficiencies arising from wage bargaining distortions and analyze two policy tools—hiring subsidies and firing penalties—that could help restore efficiency. Finally, Section 6 concludes.

2 Motivating facts

In this section, we document two novel stylized facts that challenge standard search-and-matching theories. First, we show that the direction of Beveridge curve shifts is *state-dependent*: while matching efficiency improvements typically shift the curve inward, this relationship reverses during high-efficiency periods, generating outward shifts. Second, we find that this reversal is driven by a *positive co-movement* between matching efficiency and job separation rates. This suggests that "churn" is an endogenous response to market fluidity, a feature absent in exogenous separation models.

To establish these facts, we analyze United States data covering the period from January 1978 to June 2025. We begin by detailing the construction of our key series.

Labor market data. The vacancy rate v_t is measured using the composite Help-Wanted Index of Barnichon (2010), harmonized with JOLTS to construct a continuous vacancy series. The baseline unemployment measure u_t is the headline unemployment rate (U-3, LNS14000000, BLS). We also construct an alternative measure of unemployment that treats non-employed individuals as job seekers, defining $\tilde{u}_t = u_t + \frac{p_t^{IE}}{p_t^{UE}} i_t$, where p_t^{IE} and p_t^{UE} denote the transition probabilities from inactivity and unemployment into employment, respectively, and i_t is the inactivity rate. Our baseline separation rate is obtained from the employment-to-unemployment (EU) transition probability, seasonally adjusted using CPS microdata following Elsby, Hobijn, and Şahin (2015).[1]

Matching efficiency. We measure matching efficiency following Petrongolo and Pissarides (2001) as the residual of a standard Cobb-Douglas matching function $m_t(\mu_t, u_t, v_t) = \mu_t u_t^{\sigma} v_t^{1-\sigma}$. Dividing by unemployment yields the job-finding probability f_t, which we log-linearize as:

$$\ln f_t = \ln \bar{\mu} + (1 - \sigma) \ln(\theta_t) + \varepsilon_t, \tag{1}$$

[1] Appendix B describes the derivation of the transition probabilities. For robustness, we also perform the analysis using an inflow rate to unemployment accounting for transitions from both employment *and* inactivity.

where $\theta_t = v_t/u_t$ is labor market tightness. The fitted residual ε_t serves as our time-varying measure of matching efficiency $\ln \hat{\mu}_t$.

Shifts in the Beveridge curve. We derive the Beveridge curve from the standard law of motion of unemployment, $u_{t+1} = u_t + s_t - (1 - s_t) \cdot m(\mu_t, u_t, v_t)$. Solving for vacancies yields the Beveridge curve relationship $v_t = v(u_t, \mu_t, s_t, \Delta u_{t+1})$. To capture the empirical dynamics, we estimate the following log-linear specification:

$$\ln(v_t) = \beta_c + \beta_u \ln(u_t) + \beta_m \ln \hat{\mu}_t + \beta_s \ln(s_t) + \beta_{\Delta_u} \Delta \ln(\hat{u}_{t+1}) + e_t. \tag{2}$$

We define the "Beveridge curve shift" as the component of vacancies orthogonal to unemployment movements: $\ln(v_t) - \hat{\beta}_c - \hat{\beta}_u \ln(u_t) - \beta_{\Delta_u} \Delta \ln(\hat{u}_{t+1})$.

Table 1 presents the baseline results. Consistent with standard theory, the average effect of matching efficiency is to shift the curve inward ($\beta_m < 0$), while separations shift it outward ($\beta_s > 0$). However, as we show in the decomposition analysis (see Table 3 below), this average effect masks the *state-dependent reversal* described in our first stylized fact: during periods of high matching efficiency, the strong positive response of endogenous separations (the churning channel) overwhelms the direct efficiency gain, resulting in a net outward shift.

Detrending methodology. To focus on cyclical movements and isolate business-cycle dynamics from long-run structural trends in our series, we detrend the estimated Beveridge curve shifts, matching efficiencies, and separation rates using the Rotemberg (1999) filter. This filter offers an advantage over the standard HP filter: it explicitly orthogonalizes trend and cycle components by construction. This ensures that our estimated effects of matching efficiency and separations on Beveridge curve shifts are not a byproduct from spurious trend-cycle correlation mechanically induced by the HP filter, but rather reflect genuine cyclical labor market dynamics independent of any low-frequency structural changes. Our headline results also hold when detrending with Hodrick–Prescott Hodrick and Prescott (1997) filters (see Appendix B) or when variables are regressed in levels; these robustness checks are reported in Appendix B.

Figure 1 presents the detrended cyclical components of the Beveridge curve shifts (left panel), matching efficiency (center panel), and separation rate (right panel) for

Table 1: Beveridge curve regressions

	Specification		
	(1)	(2)	(3)
Dependent Var.: Vacancy Rate v_t	**Baseline**	**Without controls**	**With inactive searchers**
Matching efficiency	-1.096***		-0.864***
	(0.090)		(0.091)
Separation rate (s_t)	1.041***		1.126***
	(0.090)		(0.093)
Unemployment (u_t)	-1.234***	-0.628***	-0.867***
	(0.058)	(0.032)	(0.035)
$\Delta \ln u_{t+1}$	-2.774***	-0.602***	-2.121***
	(0.224)	(0.151)	(0.180)
Constant	✓	✓	✓

Note: Monthly U.S. data from January 1978 to July 2025. The dependent variable is the log vacancy rate. Column (1) presents the baseline specification including matching efficiency and the separation rate as control variables in addition to log unemployment and the one-month-ahead change in log unemployment. Column (2) excludes matching efficiency and separations, reporting only the raw relationship between vacancies and unemployment. Column (3) uses separation and matching efficiency measures which account for inactive job seekers. Matching efficiency is constructed as the residual from a log matching-function regression of the job-finding rate on labor-market tightness (with column (3) using a generalized tightness measure based on effective searchers). The separation rate is constructed from CPS-based continuous-time adjusted transition hazards (employment into unemployment in columns (1) and (2); a broader measure combining separations from employment and nonparticipation in column (3)). Standard errors are conventional i.i.d. OLS standard errors. Significance levels: *** $p < 0.01$, ** $p < 0.05$, * $p < 0.10$.

both baseline and alternative measures. The baseline measures use employment-to-unemployment (E→U) flows and standard labor market tightness (v_t/u_t), while the alternative measures incorporate combined employment and inactivity-to-unemployment (E∪N→U) flows and effective-searcher tightness ($v_t/\tilde{u}_t$) to account for job search by the inactive. These detrended series capture the cyclical movements in the Beveridge curve originating from matching efficiency and the separation rate, represented by the terms $\beta_m \ln(\hat{\mu}_t)$ and $\beta_s \ln(\hat{s}_t)$, respectively, as well as unexplained movements due to the error term e_t in equation (2). The figure illustrates that both measurement approaches yield qualitatively similar cyclical patterns, reinforcing the robustness of our findings.

To complement the cyclical analysis in Figure 1, we construct Figure 2, which displays 13-month centered moving averages of the *level* series (i.e., without detrending) of Beveridge curve shifts, matching efficiency, and separations. This moving average smoothing removes high-frequency noise while preserving both cyclical and trend movements, making it easier to identify major shift episodes and their duration. Whereas Figure 1 isolates business-cycle fluctuations by removing low-frequency trends, Figure 2 retains these longer-run movements and highlights the six largest shift intervals identified in Table 2 with colored segments.

Table 2 identifies the six largest shift episodes by searching the full sample for intervals with the biggest absolute change in the Beveridge curve shift measure between start and end dates. The table reports the magnitude of each shift (column 1), together with the difference in matching efficiency (column 2) and the job separation rate (column 3) from their respective means over the preceding 48 months. The largest shift in our sample is the outward movement during December 2019–March 2020, with a magnitude of 2.61 log points, coinciding with the onset of the COVID-19 pandemic. The subsequent inward shift during May 2021–March 2023 (magnitude -0.70 log points) reflects the labor market recovery. The remaining episodes include the April 2020–September 2020 period (-0.47 log points), the Great Recession period March 2008–January 2010 (0.41 log points), and two earlier episodes in August 2000–July 2001 (0.33 log points) and July 1988–May 1990 (-0.31 log points).

According to our estimates in Table 1, on average across the full sample period, improvements in matching efficiency shift the Beveridge curve inward, while increases in the job separation rate shift it outward. However, the entries in Table 2 reveal a more nuanced pattern for the largest shift episodes. Specifically, outward shifts are predominantly associated with positive changes in the job separation rate relative to the preceding 48-month mean (e.g., +0.67 in Dec 2019–Mar 2020, +0.20 in Mar 2008–Jan 2010), while inward shifts are predominantly associated with declines in the separation rate (e.g., -0.15 in May 2021–Mar 2023, -0.10 in Jul 1988–May 1990). The April 2020–September 2020 period is notable as an exception, exhibiting both elevated matching efficiency (+0.31) and elevated separations (+0.52) alongside an inward shift. Overall, these results reinforce the central role of separation rate dynamics in driving the largest Beveridge curve shifts.

We next decompose the channels through which matching efficiency and job sepa-

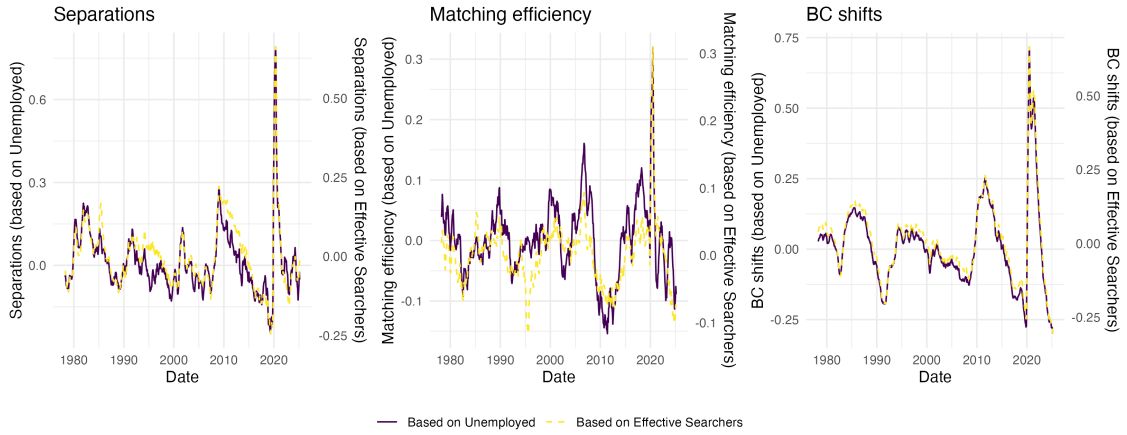

Figure 1: Detrended Beveridge curve shifts, matching efficiency, and separation rates

Note: This figure displays the cyclical components of Beveridge curve shifts (left panel), matching efficiency (center panel), and separation rates (right panel), detrended using the Rotemberg (1999) filter. Each panel shows two series: (i) *Baseline* measures computed using employment-to-unemployment (E→U) flows and standard tightness (v_t/u_t), and (ii) *Alternative* measures computed using combined employment *and* inactivity-to-unemployment (E∪N→U) flows and effective-searcher tightness ($v_t/\tilde{u}_t$), where $\tilde{u}_t$ includes inactive job seekers weighted by their job-finding rates relative to the unemployed. The detrending isolates business-cycle fluctuations from long-run structural trends. Sample period: Jan 1978 to Jun 2025. Data source: FRED, JOLTS, and CPS.

Figure 2: Beveridge curve shifts over time.

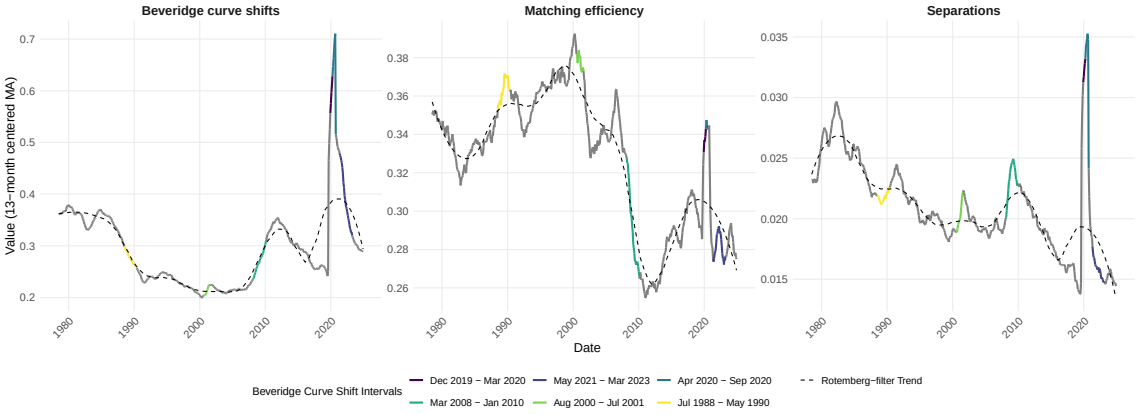

Note: This figure shows 13-month centered moving averages of Beveridge-curve shifts, matching efficiency, and separations from Jan 1978 to Jun 2025. The smoothing helps reveal underlying trends by reducing high-frequency noise. The colored segments highlight the top 6 shift intervals identified in the table, with each color corresponding to a specific interval. Gray segments indicate periods outside these major shift episodes. The three panels display (left to right): BC shifts computed as deviations in the vacancy-unemployment relationship, matching efficiency, and separation rates. Data source: FRED, JOLTS, and CPS.

rations affect Beveridge curve shifts. A key insight from our theoretical framework is that matching efficiency can induce endogenous separations: higher matching ef-

Table 2: Top Beveridge-curve shift intervals

Interval	**BC shift (end-start)**	**Matching efficiency vs prior 48m (mean diff)**	**Separations vs prior 48m (mean diff)**
Dec 2019 – Mar 2020	2.61	-0.08	0.67
May 2021 – Mar 2023	-0.70	-0.09	-0.15
Apr 2020 – Sep 2020	-0.47	0.31	0.52
Mar 2008 – Jan 2010	0.41	-0.17	0.20
Aug 2000 – Jul 2001	0.33	0.02	0.01
Jul 1988 – May 1990	-0.31	0.07	-0.10

Note: This table presents the top 6 Beveridge-curve shift intervals, ranked by the absolute magnitude of the shift (—BC shift (end-start)—). Each interval represents a period during which the Beveridge curve exhibited a notable shift. The BC shift is computed as the difference in log vacancy rates between the end and start of the interval. Matching efficiency and separations are compared to the 48-month period immediately preceding each interval. Matching efficiency (baseline matching efficiency) measures the residual efficiency of the job-matching process, while separations (the baseline separation rate from flows) capture the flow rate from employment (and nonparticipation) into unemployment. The sample period is Jan 1978 to Jun 2025. Data source: FRED, JOLTS, and CPS.

ficiency reduces the expected cost of filling a vacancy, encouraging firms to create jobs but also lowering the value of marginal matches, potentially triggering more job destruction. To isolate these two channels empirically, we decompose the total effect of matching efficiency into (i) the component that operates through induced separations, and (ii) the residual component orthogonal to separations, which captures the direct matching effect holding separations constant. This decomposition is implemented via a first-stage regression of matching efficiency on separations (including CPS inactivity-flow controls), with the fitted values capturing the endogenous separation channel and the residuals capturing the orthogonalized matching efficiency channel. The first-stage regression results are reported in Appendix B.

Table 3 presents regression results examining how matching efficiency and job separations affect Beveridge curve shifts. Columns (1) and (2) report results for the full sample, while columns (3) and (4) restrict attention to periods when matching efficiency exceeds the 67th percentile (i.e., high matching efficiency periods). Columns

(1) and (3) regress BC shifts on matching efficiency alone, while columns (2) and (4) implement the channels decomposition, separating the total effect into the endogenous separation channel and the orthogonalized matching efficiency channel.

Table 3: Beveridge curve shifts, matching efficiency, and job separation

	Beveridge Curve Shifts		Beveridge Curve Shifts when ME $\geq$ 67th pctile(ME)	
	(1) Matching Efficiency	(2) Channels	(3) Matching Efficiency	(4) Channels
Matching Efficiency	-0.261***		0.424***	
	(0.080)		(0.134)	
Separations		0.613***		0.605***
		(0.034)		(0.065)
Matching Efficiency orthogonalized to Separations		-0.467***		-0.112
		(0.063)		(0.128)
Constant	-0.449***	-0.306***	-0.592***	-0.597***
	(0.107)	(0.078)	(0.160)	(0.140)
Observations	570	570	190	190

Note: Monthly U.S. data from January 1978 to June 2025. The dependent variable is the Beveridge curve shift. Columns (1) and (3) report regressions of BC shifts on matching efficiency. Columns (2) and (4) report the channels decomposition: BC shifts regressed on separations and matching efficiency orthogonalized to separations. Columns (1)–(2) use the full sample, while columns (3)–(4) restrict to periods of large shifts, defined as observations where matching efficiency exceeds the 67th percentile (i.e., high matching efficiency periods). All variables are standardized. The decomposition is implemented via a first-stage regression of matching efficiency on separations (including CPS inactivity-flow controls), with the fitted values capturing the endogenous separation channel and the residuals capturing the orthogonalized matching efficiency channel. The second-stage regressions control for log unemployment and CPS inactivity-flow transitions (p_{UN}, p_{NU}, p_{EN}, p_{NE}); coefficients on these controls are suppressed. Standard errors are conventional i.i.d. OLS standard errors. Significance levels: *** $p < 0.01$, ** $p < 0.05$, * $p < 0.10$.

The full-sample results in column (1) show that matching efficiency exhibits a negative coefficient (-0.261), consistent with the standard view that improvements in matching efficiency shift the Beveridge curve inward. The channels decomposition in column (2) reveals that separations have a positive coefficient (0.613), shifting the curve outward, while matching efficiency orthogonalized to separations has a negative coefficient (-0.467). However, columns (3) and (4) reveal a striking reversal during

high matching efficiency periods. Column (3) shows that the overall matching efficiency effect becomes positive (0.424), implying that increases in matching efficiency shift the Beveridge curve *outward* rather than inward during these periods. Column (4) demonstrates that this reversal occurs because the endogenous separation channel (captured by the separations coefficient of 0.605) dominates the direct matching effect (captured by the orthogonalized matching efficiency coefficient of -0.112), highlighting the critical role of endogenous separation dynamics in driving Beveridge curve shifts during periods of elevated matching efficiency.

To summarise, in this section we have shown that the Beveridge curve typically shifts inward when matching efficiency increases. However, the shift direction is non-linear and state-dependent. When matching efficiency increases are accompanied by separation rate increases, the Beveridge curve shifts outward. In the following sections, we show how a standard non-linearly and globally solved DMP model with endogenous job destruction in the spirit of Mortensen and Pissarides (1994) can capture these features and their implications.

3 Theoretical framework

Definition 1 (Beveridge curve)**.**
Fix a reduced-form mapping from matching efficiency m to the gross separation rate, denoted $s^\star(m) \in (0,1)$. The Beveridge curve is the locus $B(m)$ of unemployment–vacancy pairs $(u,v) \in \mathbb{R}_+ \times \mathbb{R}_+$ satisfying

$$\frac{M(u,v)}{1-u} = \frac{1}{m}\frac{s^\star(m)}{1-s^\star(m)}. \tag{3}$$

Equation (3) nests the canonical Beveridge curve. In standard models with exogenous separations, $s^\star(m)$ is constant, while in models with endogenous job destruction, $s^\star(m)$ inherits equilibrium feedback through the job-destruction cutoff and market tightness.

Rearranging (3) yields

$$\frac{M(u,v)}{1-u} = \frac{1}{m}\frac{s^\star(m)}{1-s^\star(m)} = -\frac{1}{m} + \frac{1}{m(1-s^\star(m))}. \tag{4}$$

Since the left-hand side is strictly increasing in v for any fixed u, an increase in the right-hand side corresponds to an outward shift of the Beveridge curve (higher v required to support a given u).

Differentiating the right-hand side with respect to m yields the decomposition

$$\frac{\partial}{\partial m}\left(-\frac{1}{m}+\frac{1}{m(1-s^\star(m))}\right)=-\frac{1}{m^2}\frac{s^\star(m)}{1-s^\star(m)}+\frac{1}{m(1-s^\star(m))^2}\frac{ds^\star(m)}{dm}, \tag{5}$$

where the first term is the *direct hiring effect* and the second term is the *endogenous churning effect*.

Theorem 1 (Condition for outward shifts)**.**
An increase in matching efficiency shifts the Beveridge curve outward if and only if

$$\frac{d\log s^\star(m)}{d\log m}>1-s^\star(m). \tag{4}$$

Proof. Define $B(m)\equiv-\frac{1}{m}+\frac{1}{m(1-s^\star(m))}$. An outward shift is equivalent to $dB(m)/dm>0$. Differentiating $B(m)$ and rearranging yields that $dB(m)/dm>0$ if and only if

$$\frac{1}{1-s^\star(m)}\frac{ds^\star(m)}{dm}>\frac{s^\star(m)}{m}. \tag{5}$$

Multiplying both sides by $m/s^\star(m)$ gives

$$\frac{d\log s^\star(m)}{d\log m}>1-s^\star(m), \tag{6}$$

which is (4). ■

When m increases, the expected cost of filling a vacancy falls, increasing the firm's outside option. Consequently, firms become more selective, raising the reservation productivity threshold. If the density of matches near this threshold is high, the resulting surge in separations, captured by the elasticity term in Theorem 1, overwhelms the faster hiring speed. This result explains the "efficiency paradox" observed in post-COVID data: the labor market was highly fluid, but this very fluidity encouraged a rate of labor turnover that kept unemployment elevated relative to vacancies.

Corollary 1 (Exogenous separation)**.**

If separations are exogenous, $s^\star(m)$ is constant in m and the Beveridge curve shifts inward when m increases.

Corollary 1 provides a useful benchmark. If separations do not respond to matching efficiency, then the churning margin is shut down: improvements in m only speed up job creation, without inducing additional job destruction. In that case, the Beveridge curve shifts inward unambiguously. The corollary thus highlights that the sign reversal documented in the data—and rationalized in our model—requires separations to endogenously co-move with matching conditions.

Proof. In the exogenous job separation model, the separation rate is constant, so $\frac{\partial \log(s(m))}{\partial \log(m)} = 0$. This implies that the elasticity of the job separation rate with respect to matching efficiency is always lower than the survival rate, and the condition in Theorem 1 never holds. ■

4 Baseline model

Our model formulation is consistent with the most commonly employed versions of the Diamond-Mortensen-Pissarides Model formulated in (Mortensen and Pissarides, 1994; Den Haan, Ramey, and Watson, 2000; Yashiv, 2007; Hagedorn and Manovskii, 2008). Time is discrete. Firms produce outputs only using labor inputs. The firms post vacancies to be matched with unemployed workers in a labor market characterized by search frictions.

Timing A worker searches for a vacancy, and firms post vacancies. The two sides are matched based on a matching function. After matching, an exogenous separation shock arises within the same period. Then, at the beginning of the following period, a firm endogenously determines whether to lay off the worker. After passing the endogenous layoff condition, the worker bargains the wage and produces output. The timing is summarized in Figure 3.

Matching function Following Den Haan, Ramey, and Watson (2000), we consider

Figure 3: Timing in the model

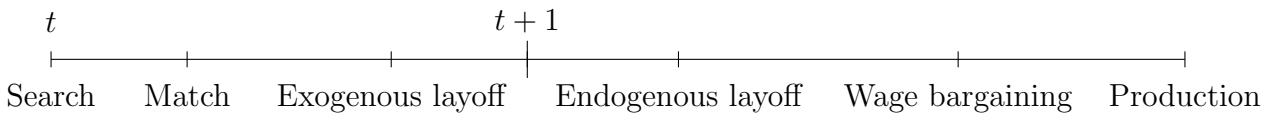

the following CRS matching function:[2]

$$M(m, V, U) = m\frac{UV}{(V^{\xi} + U^{\xi})^{\frac{1}{\xi}}} \ . \tag{7}$$

The number of new matches M in the economy is determined by the number of vacancies V posted by firms, the number of unemployed workers U searching to fill these vacancies, and matching efficiency m. Based on the matching function, we define the job finding rate p and vacancy filling rate q as follows:

$$p(\theta) := m\theta(1 + \theta^{\xi})^{-\frac{1}{\xi}} \tag{8}$$

$$q(\theta) := m(1 + \theta^{\xi})^{-\frac{1}{\xi}}, \tag{9}$$

where $\theta := \frac{V}{U}$ is the market tightness.

Aggregate states The aggregate states S are composed of exogenous and endogenous parts. The exogenous component is the aggregate TFP level A and the matching efficiency m. The endogenous part is the prior period's incumbent and newly matched workers n^*_{-1}.

$$S = \left\{A, m, n^*_{-1}\right\} \tag{10}$$

The log aggregate TFP follows an AR(1) process:

$$log(A') = \rho_A log(A) + \sigma_A \epsilon, \quad \epsilon \sim_{iid} N(0, 1). \tag{11}$$

[2]We also consider a Cobb-Douglas CRS matching function as a robustness check for our main results, which does not change significantly from the baseline.

The log aggregate matching efficiency also follows an AR(1) process:

$$log(m') = (1-\rho_m)log(\overline{m}) + \rho_m log(m) + \sigma_m \epsilon, \quad \epsilon \sim_{iid} N(0,1), \tag{12}$$

where $\overline{m}$ is the unconditional average the matching efficiency. The current working population n is endogenously determined by the following law of motion:

$$n(S) = (1-\lambda)(1-H(S))(n^*_{-1}) \tag{13}$$

$$n^*(S) = n(S) + v(S)q(\theta(S)) \tag{14}$$

where λ is the exogenous separation rate. $H(S)$ is the endogenous separation rate set by firms' endogenous job destruction decisions.

Household We consider a representative household that is composed of a continuum of unit measures of labor forces. The employed portion of the labor force earns wages, and the unemployed portion engages in home production, all of which are treated as labor income $W(S)$. The household holds the claim for the dividend $D(S)$ and saves for future dividend claims. Thus, the budget constraint is as follows:

$$c + a' = W(S) + D(S) + \underbrace{(a - D(S))}_{\text{Ex-dividend equity value}} \tag{15}$$

where a is the value of the dividend claim. The apostrophe indicates the future variables. The household has a temporal CRRA utility and discounts future by $\beta \in (0,1)$. The recursive formulation of the households' problem is as follows:

$$V(a;S) = \max_{c,a'} \quad \frac{c^{1-\sigma}}{1-\sigma} + \beta \mathbb{E} V(a';S') \tag{16}$$

$$\text{s.t.} \quad c + a' = W(S) + D(S) + (a - D(S)) \tag{17}$$

Real values of employment and unemployment A continuum of a unit measure of ex-ante homogenous labor force is considered. Their labor productivity z is distributed as follows:

$$z \sim_{iid} N(1, \sigma_z) \tag{18}$$

Matched individuals get a new productivity drawn in every period. When a worker is employed, they earn wage. Then, an exogenous Poisson separation shock arrives at a rate of $\lambda \in (0,1)$. The worker continues to stay in the match in the following period with a probability of $(1-\lambda)$ or searches for another job with probability λ and gets matched with a new job with a probability of $p = p(\theta(S))$. In the following period, a firm decides whether to lay off the worker, which is captured by endogenous separation rate $H(S')$. All workers are assumed to participate in job search when unemployed. All the future values are discounted by the stochastic discount factor $\mu(S, S')$. In equilibrium, the wage is determined by Nash bargaining, resulting in $w = w(z; S)$. We define the value function of an employed worker earning the equilibrium wage $v^e(z; S)$ and the value function of an unemployed worker $v^u(z; S)$ as follows:

$$
\begin{aligned}
&v^e(z;S) = w(z;S) \\
&+ ((1-\lambda) + \lambda p(\theta(S)))\mathbb{E}\left[\mu(S,S')(1-H(S'))(v^e(z';S') - v^u(z';S'))\middle| J(z';S') > 0\right] \\
&+ \mathbb{E}\left[\mu(S,S')v^u(z';S')\right] \qquad (19) \\
&v^u(z;S) = b + p(\theta(S))\mathbb{E}\left[\mu(S,S')(1-H(S'))(v^e(z,w';S') - v^u(z';S'))\middle| J(z';S') > 0\right] \\
&+ \mathbb{E}\left[\mu(S,S')v^u(z';S')\right] \qquad (20)
\end{aligned}
$$

When a worker starts a period as unemployed, the worker engages in home production $b > 0$ and searches for a job to be matched with a vacancy with the probability $p = p(\theta(S))$.

Firms (=jobs) A firm (job) produces output using a CRS Cobb-Douglas function with only a labor input.[3] In equilibrium, the wage is determined as $w = w(z; S)$ by Nash bargaining. Based on this, we define the value function J of a firm that pays out the equilibrium wage, $J(z; S)$:

$$
J(z;S) = Az - w(z;S) + (1-\lambda)\mathbb{E}\left[\mu(S,S')(1-H(S'))J(z';S')|J(z';S') > 0\right] \qquad (21)
$$

where $\mu(S, S')$ is the stochastic discount factor. At the beginning of a period, a firm decides whether to destruct a job based on the following individual rationality condition: $J(z; S) > 0$. It is worth noting that all the value functions are written at the

[3]The CRS production allows the firm-level characterization to boil down to the job-level characterization as in other models in the literature.

timing after the job destruction decision, which eases the wage bargaining characterization. We define the endogenous job destruction probability $H(S)$ accordingly:

$$H(S) := \mathbb{P}\left(J(z;S) < 0\right). \tag{22}$$

Wage bargaining A matched worker with productivity z and the firm determine the wage by Nash bargaining. The worker's bargaining power is $\eta > 0$. The standard Nash bargaining leads to the following condition where the wage is determined:

$$(1-\eta)(v^e(z;S) - v^u(z;S)) = \eta J(z;S) \tag{23}$$

Detailed derivation of this condition is available in the Appendix.

Equilibrium conditions In equilibrium, we require the following conditions:

$$\text{[Free entry]} \quad \kappa = q(\theta(S))(1-\lambda)\mathbb{E}\left[\mu(S,S')(1-H(S'))J(z';S')|J(z';S') > 0\right] \tag{24}$$

$$\text{[Agg. output]} \quad Y(S) = A\int_{J(z;S)>0} z d\Phi + b\int_{J(z;S)\leq 0} d\Phi \tag{25}$$

$$\text{[Resource const.]} \quad C(S) = Y(S) - \kappa v(S) = W(S) + D(S) \tag{26}$$

The first is free entry conditions. Firms pay a cost κ when they post a vacancy. In equilibrium, a firm's expected profit and the vacancy posting cost balance. In the national account, aggregate output Y balances with the aggregate consumption C after accounting for the total vacancy posting cost. From the income side identity, the consumption is equal to the sum of labor and capital (dividend) incomes minus the lump-sum tax.

4.1 Equilibrium characterization

We characterize the equilibrium by establishing the values for wages, job creation, and crucially, the endogenous job destruction threshold.

Wage Determination. Wages are determined via Nash bargaining, sharing the surplus of the match according to the worker's bargaining power η. Using the value functions defined above, the bargaining condition $(1-\eta)(v^e(z)-v^u(z)) = \eta J(z)$ yields the equilibrium wage schedule:

$$w(z;S) = (1-\eta)b + \eta(Az + \theta\kappa). \tag{27}$$

The wage is a weighted average of the worker's outside option (home production b) and the match productivity plus labor market tightness benefits.

The Endogenous "Churning" Threshold. The core mechanism of our model lies in the firm's decision to dissolve a match. A firm destroys a job if the match value becomes negative, $J(z;S) < 0$. This defines a reservation productivity threshold $z_s(S)$ where the firm is indifferent between retaining the worker and separating:

$$z_s(S) = \frac{1}{A}\left(\underbrace{b + \frac{\eta}{1-\eta}\theta\kappa}_{\text{Outside Options}} - \underbrace{\frac{1}{1-\eta}\frac{\kappa}{q(\theta(S))}}_{\text{Hoarding Value}}\right). \tag{28}$$

Equation (28) reveals the economic trade-off governing separations. The threshold z_s increases with the worker's outside option b and market tightness θ. Crucially, it decreases with the expected hiring cost $\frac{\kappa}{q(\theta)}$. When hiring is costly (low $q(\theta)$), firms "hoard" labor, tolerating lower productivity matches (lower z_s). Conversely, when matching becomes efficient (high m, high $q(\theta)$), the cost of replacing a worker falls. This reduces the hoarding motive, raising z_s and triggering "churn."

Based on this threshold, the endogenous separation rate is the mass of employment below the cutoff:

$$H(S) = \Phi\left(\frac{z_s(S) - 1}{\sigma_z}\right). \tag{29}$$

Job Creation Condition. Firms post vacancies until the expected cost equals the expected benefit. The benefit depends on the expected surplus from a new hire, which is conditional on the new match surviving the endogenous separation cut in the next

period $(1 - H(S'))$:

$$\frac{\kappa}{q(\theta(S))} = (1-\lambda)\mathbb{E}\left[\mu(S,S')(1-H(S'))J(z';S') \mid J(z';S') > 0\right]. \tag{30}$$

Substituting the wage equation (27) into the value function $J(z)$, we obtain the fundamental Job Creation (JC) condition:

$$\frac{\kappa}{q(\theta(S))} = (1-\lambda)\mathbb{E}\left[\mu(S,S')(1-H(S'))\left((1-\eta)(A\overline{z}(S')-b) - \eta\theta\kappa + \frac{\kappa}{q(\theta(S'))}\right)\right], \tag{31}$$

where $\overline{z}(S') = \mathbb{E}[z|z > z_s(S')]$ is the average productivity of surviving matches.

Table 4 summarizes the full dynamic system governing the economy.

Description	**Equation**
Aggregate productivity	$\log(A') = \rho_A \log(A) + \sigma_A \epsilon$
Aggregate matching efficiency	$\log(m') = \rho_m \log(m) + \sigma_m \epsilon$
Endogenous Job destruction	$H = \Phi(\frac{z_s - 1}{\sigma_z})$
Matches at the start of the period	$n^* = n + vq(\theta)$
Law of motion of employment	$n = (1-\lambda)(1-H)n^*_{-1}$
Job creation condition	$\frac{\kappa}{q(\theta)} = (1-\lambda)\mathbb{E}[\mu(1-H')\left(A'\overline{z}' - \overline{w}' + \frac{\kappa}{q(\theta')}\right)]$
Job destruction condition	$Az_s = b + \frac{\eta}{1-\eta}\kappa\theta - \frac{1}{1-\eta}\frac{\kappa}{q(\theta)}$
Cond. mean match productivity	$\overline{z} = 1 + \sigma_z \frac{\phi(\frac{z_s-1}{\sigma_z})}{1-\Phi(\frac{z_s-1}{\sigma_z})}$
Bargained average wage	$\overline{w} = (1-\eta)b + \eta[A\overline{z} + \theta\kappa]$
Probability of finding a job	$p(\theta) = m\theta(1+\theta^\xi)^{-\frac{1}{\xi}}$
Probability of filling a vacancy	$q(\theta) = m(1+\theta^\xi)^{-\frac{1}{\xi}}$
Resource constraint	$C = A\overline{z}n + b(1-n) - \kappa v$
Stochastic discount factor	$\mu = \beta\left(\frac{C'}{C}\right)^{-\sigma}$
Tightness	$\theta = \frac{v}{u}$
Unemployed	$u = 1 - n$

Table 4: Summary of assumptions and equilibrium conditions

4.2 The Anatomy of the separation elasticity

We now connect the equilibrium conditions to the "Churning Channel" identified in Theorem 1. The theorem states that the Beveridge curve shifts outward if the elasticity of separations to matching efficiency is sufficiently high. Here, we derive the structural form of this elasticity.

Proposition 1 (Transmission mechanism)**.**
In the stationary equilibrium, an increase in matching efficiency m unambiguously raises the reservation productivity threshold z_s, increasing endogenous separations:

$$\frac{\partial z_s(S)}{\partial m} > 0. \tag{32}$$

Proof. An increase in m raises the vacancy filling rate $q(\theta)$ for any given θ. From the Job Destruction condition (28), a higher q reduces the expected hiring cost term ($-\frac{\kappa}{q}$ becomes less negative), directly increasing z_s. ■

This proposition confirms the intuition that easier hiring reduces labor hoarding. We can now quantify the separation elasticity $\varepsilon_{s,m}$ that governs the Beveridge curve shift. Differentiating the gross separation rate $s(m) = 1 - (1-\lambda)(1-\Phi(z_s))$, we obtain:

$$\underbrace{\frac{\partial \log s(m)}{\partial \log m}}_{\text{Elasticity } \varepsilon_{s,m}} = \underbrace{\left(\frac{(1-\lambda)\phi_z(\hat{z}_s)}{s(m)} \right)}_{\text{Density at Cutoff}} \times \underbrace{\left(\frac{\partial z_s}{\partial m} \frac{m}{\sigma_z} \right)}_{\text{Sensitivity of Cutoff}}. \tag{33}$$

Equation (33) reveals why the Beveridge curve shift is non-linear and state-dependent. The magnitude of the "churning" response depends on the density of matches at the cutoff, $\phi_z(\hat{z}_s)$.

As shown in Figure 4, this density is not constant. When the economy is in a state where z_s falls into a high-density region of the productivity distribution (the "Upward shift region"), a small improvement in matching efficiency triggers a disproportionately large wave of separations. Since productivity shocks are normally distributed, the density ϕ_z is hump-shaped. This implies that the 'churning channel' is most potent when the reservation threshold z_s is near the center of the distribution—exactly

Figure 4: Beveridge curve shifts and the matching efficiency cutoffs

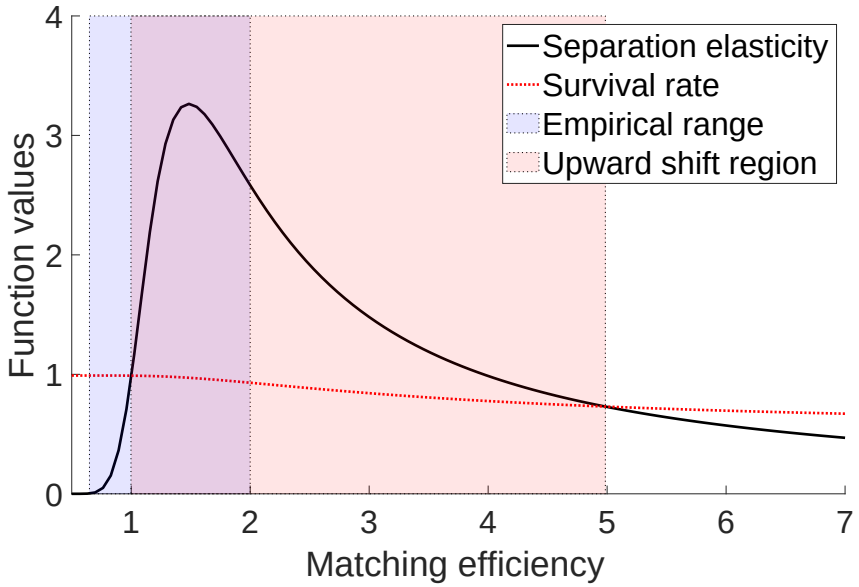

Notes: The figure illustrates the condition from Theorem 1. The black line represents the separation elasticity $\varepsilon_{s,m}$. When this elasticity exceeds the survival rate (red dotted line), the Beveridge curve shifts outward.

where the economy sits during high-efficiency recoveries. This structural feature explains why the Beveridge curve response can flip from inward to outward depending on the state of the economy.

5 Quantitative analysis

5.1 Solution method

The canonical endogenous job destruction model displays highly nonlinear global unemployment dynamics due to the endogenous destruction cutoff change in the cross-sectional skill distribution. Agents form a consistent expectation of the future dynamics to make a contemporaneous decision. In the baseline model, one of the important channels where the expectation plays a key role is the vacancy posting condition, where the state-contingent marginal benefit of vacancy posting needs to be computed. Therefore, it is necessary to sharply characterize the nonlinear functional form of the aggregate states to solve the global solution recursive competitive equilibrium globally. This difficulty has limited the global analysis of the impact of

endogenous separation on the labor market dynamics. The recent global solution method, the repeated transition method by Lee (2025), overcomes this problem in the sequence space by utilizing the recursivity of the recursive competitive equilibrium. Specifically, it utilizes the fact that all the recursive competitive equilibrium outcomes are realized on a simulated exogenous shock path if the simulated path is long enough, forming an ergodic set of all the possible aggregate allocations. Then, by identifying and combining the last iteration's value (policy) functions of the period with the aggregate states realized to be closest to the future states, the conditional expectation can be accurately computed in each period. The detailed implementation is elaborated in the Appendix.

One of the important contributions of this paper is solving for the global equilibrium path with the Hosios condition, which serves as an efficient benchmark to the baseline model. The Hosios condition requires the worker's bargaining power to fluctuate over the business cycle, which affects the business cycle fluctuation, leading to a complex fixed-point problem. The repeated transition method overcomes this problem by simultaneously updating the sequence of bargaining power with the other equilibrium allocation paths over the iterations, achieving uniform convergence to the true equilibrium path. In Section 5, we extensively analyze the Hosios-implied equilibrium path in comparison to the baseline model and its policy implications.

5.2 Calibration Strategy

We calibrate the model at a monthly frequency to match key first and second moments of the U.S. labor market. Our strategy distinguishes between standard structural parameters, which are set to values common in the literature, and mechanism-specific parameters, which are calibrated to match the volatility of unemployment and vacancies.

Table 5 summarizes the parameter values. Parameters marked with an asterisk (*) are internally calibrated to minimize the distance between model-generated moments and their empirical counterparts.

Standard Parameters. We set the discount factor β to match an annualized interest rate of 4%. The matching function elasticity ξ is set to 0.7, consistent with standard estimates. The exogenous separation rate λ is fixed at 0.01, attributing the

Table 5: Calibrated Parameters

Parameters	Description	Value
Basic parameters		
b	Unemployment benefit*	0.5018
κ	Vacancy posting cost*	0.7993
m	Average matching efficiency*	1.3743
σ_z	Idiosyncratic productivity dispersion*	1.1000
λ	Exogenous separation rate	0.0100
ξ	Matching function parameter	0.7000
β	Household's discount factor	0.9966
η	Worker's bargaining power	0.4455
Aggregate shock parameters		
ρ_A	Aggregate productivity shock persistence	0.9830
σ_A	Aggregate productivity shock volatility*	0.0330
ρ_m	Matching efficiency shock persistence*	0.9770
σ_m	Matching efficiency shock volatility*	0.0400

Note: Parameters marked with an asterisk (*) are jointly calibrated to match the targets in Table 6.

remainder of labor turnover to the endogenous channel.

Targeted Moments and Identification. Table 6 reports the target moments used to discipline the model's dynamic behavior. We construct the empirical moments using U.S. data extended from 1955 to 2024. Vacancies are measured using the composite Help-Wanted Index (Barnichon, 2010), harmonized with JOLTS data. Unemployment and job-finding rates are constructed from BLS data following the methodology of Shimer (2005).

The calibration of the shock processes is critical for quantitative realism. We employ a two-step approach:

1. **Matching Efficiency Process:** We estimate the stochastic process for matching efficiency directly from the data using a Kalman filter, following Sedláček (2014). This treats matching efficiency as an unobserved component driving

the wedge in the matching function, identified by variations in the vacancy, unemployment, and hire rates.

2. **TFP and Productivity Dispersion:** Given the estimated matching efficiency process, we calibrate the TFP volatility σ_A and the idiosyncratic productivity dispersion σ_z to match the observed volatilities of unemployment and vacancies.

Crucially, the idiosyncratic dispersion parameter σ_z determines the shape of the productivity distribution $F(z)$. By governing the density of matches near the reservation threshold z_s, σ_z dictates the sensitivity of endogenous separations to aggregate shocks. A precise calibration of this parameter is therefore essential to capture the "churning channel" accurately. We solve the model globally by discretizing the TFP process into 11 grid points (covering ± 3 standard deviations) and the matching efficiency process into 3 grid points (covering ± 1 standard deviation) using the Tauchen method.

Table 6: Calibration Targets vs. Model Moments

	Model	Data	Reference
Steady-state			
Unemployment rate u_{ss}	0.050	0.050	Bureau of Labor Statistics (BLS)
Vacancy posting rate v_{ss}	0.037	0.037	Bureau of Labor Statistics (BLS)
Job-finding rate p_{ss}	0.433	0.433	Bureau of Labor Statistics (BLS)
Business cycle			
Unemp. volatility $s.d.(u_t)$ ($p.q.$ in %)	10.584	11.400	Bureau of Labor Statistics (BLS)
Vacancy volatility $s.d.(v_t)$ ($p.q.$ in %)	14.720	12.440	Bureau of Labor Statistics (BLS)
Matching eff. shock persistence* ρ_{ME}	0.977	0.977	Sedláček (2014)
Matching eff. shock volatility* σ_{ME}	0.040	0.040	Sedláček (2014)

Notes: Model moments are computed from the ergodic distribution of the global solution. Data sources: BLS (LNS13000000, LNS14000000) and Barnichon (2010).

5.3 The Equilibrium Beveridge Curve: Validating the Paradox

We now examine the global nonlinear solution to determine if the "churning channel" identified in Theorem 1 is quantitatively sufficient to generate the observed Beveridge

curve dynamics. Figure 5 displays the equilibrium relationship between unemployment and vacancies for the baseline model (Panel a) and the exogenous separation counterfactual (Panel b), where points are color-coded by the state of matching efficiency.

The contrast between the two models confirms our theoretical predictions regarding the "efficiency paradox." In the baseline model with endogenous separations (Panel a), periods of high matching efficiency (indicated by blue squares) are associated with a distinct *outward* shift of the curve. Despite the ease of hiring, the equilibrium settles at higher unemployment and vacancy rates. This confirms that the elasticity condition in Theorem 1 holds in our calibration: the surge in endogenous separations outweighs the direct efficiency gain. In sharp contrast, the counterfactual model with exogenous separations (Panel b) shows that high matching efficiency always shifts the curve *inward*. Without the endogenous separation margin, easier hiring unambiguously lowers unemployment for any given vacancy level, failing to replicate the non-monotonic dynamics observed in the post-COVID data.

Notably, the baseline model with endogenous separation produces a coherent Beveridge curve relationship, contrary to the finding in the seminal contribution by Fujita and Ramey (2012). This difference underscores that the appearance, or absence, of a Beveridge curve in endogenous separation models can be sensitive to the solution method. Our global nonlinear approach accurately captures the reservation productivity dynamics and the associated endogenous separations, yielding a realistic negative unemployment-vacancy relationship that shifts with matching efficiency.

To precisely quantify this non-linearity, Figure 6 plots the conditional average of the Beveridge curve for each efficiency state. In the baseline model (Panel a), the curve shifts outward significantly as efficiency rises. This captures the non-monotonic nature of the relationship: matching efficiency improves the trade-off up to a point, but eventually triggers excessive churn that worsens the trade-off.

The static outward shift has profound dynamic consequences for the economy's stability. Because high matching efficiency raises the reservation productivity threshold z_s, it leaves the economy with a fragile distribution of matches that are highly sensitive to negative shocks. Figure 7 illustrates this by plotting the generalized impulse response (GIRF) of unemployment to a negative TFP shock across different states. When

Figure 5: Beveridge curve dynamics: Endogenous vs. Exogenous Separation

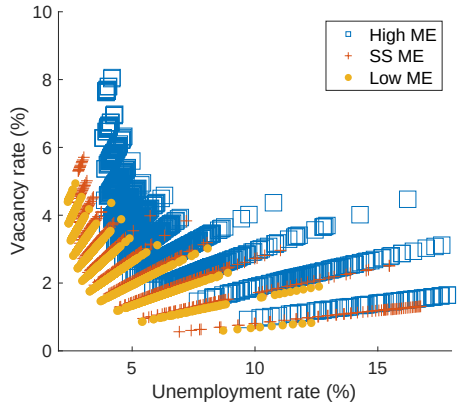

(a) Baseline: Paradoxical Outward Shift Shift

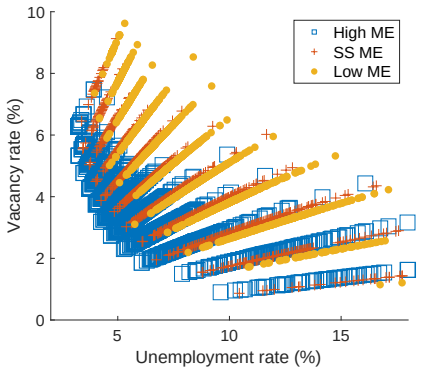

(b) Exogenous JD: Standard Inward

Notes: The figure plots the joint distribution of unemployment and vacancies from the global solution. Blue squares denote periods of high matching efficiency (+1 s.d.), while yellow crosses denote low efficiency (−1 s.d.).

Figure 6: Nonlinear shifts of the Beveridge curve: conditional averages

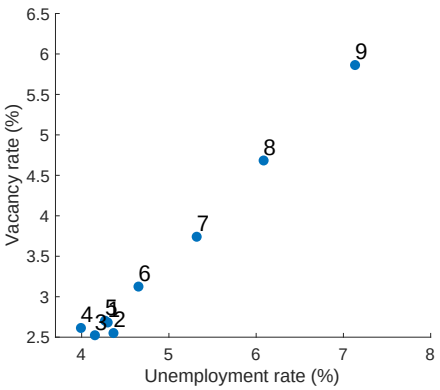

(a) Baseline

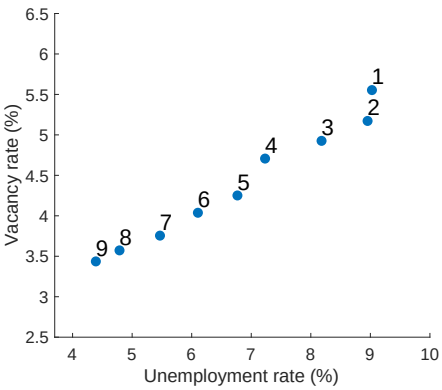

(b) Exogenous JD

the shock hits during a high-efficiency period (Panel a), the unemployment response is significantly amplified. The initial mass of marginal workers is high due to the elevated reservation threshold, leading to a sharp wave of separations when productivity falls. Conversely, when efficiency is low (Panel b), the economy exhibits "labor hoarding" behavior; firms are already reluctant to separate due to high replacement costs, rendering the unemployment response more resilient to the shock. This state-dependence explains why recessions occurring during fluid labor market conditions can exhibit sharper unemployment spikes than those during stagnant periods.

Figure 7: State-dependent unemployment responses to a negative TFP shock

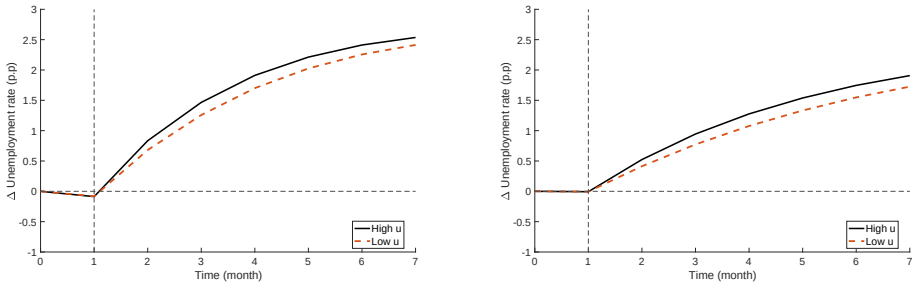

(a) Response during High ME (Fragile)

(b) Response during Low ME (Resilient)

Finally, we assess the model's ability to reproduce historical volatility patterns. Figure 8 compares the model-implied unemployment series against U.S. data (dashed red line). The baseline model (Panel a) successfully captures the large spikes in unemployment volatility observed in the data, particularly during the high-efficiency episodes shaded in blue. In contrast, the exogenous separation model (Panel b) predicts a counterfactually smooth unemployment path. By shutting down the churning channel, the exogenous model misses the explosive nature of unemployment during reorganization episodes. This confirms that endogenous separations are not merely a theoretical mechanism but a quantitative necessity for tracking the volatility of U.S. labor market dynamics.

Figure 8: Model Fit: Matching Historical Volatility

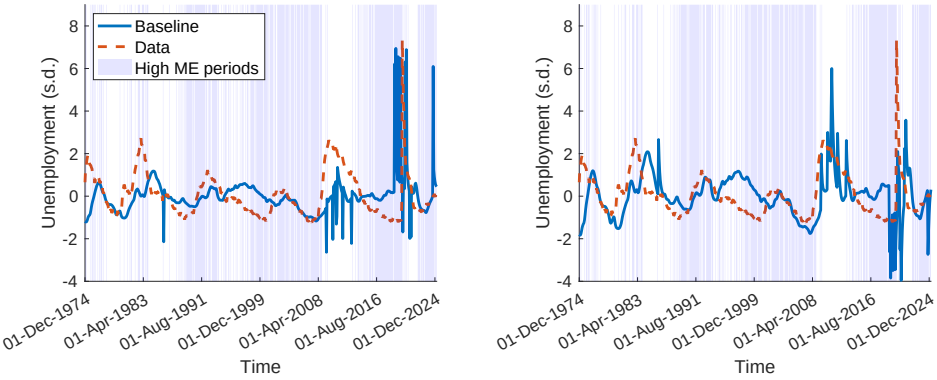

(a) Baseline (Endogenous Sep)

(b) Counterfactual (Exogenous Sep)

6 Efficiency and policy analysis

Theorem 1 shows that high matching efficiency can raise endogenous separations through the churning channel, generating outward Beveridge-curve shifts. This section asks whether the resulting volatility is efficient, and if not, what simple instruments can mitigate it.

6.1 A constrained-efficient benchmark: the Hosios path

In canonical search models, the decentralized equilibrium is constrained efficient when the surplus-sharing rule internalizes the matching congestion externality (Hosios, 1990). Formally, efficiency requires the worker's bargaining weight to equal the unemployment elasticity of the matching function:

$$\eta_t^* = \frac{\partial M(U_t, V_t)}{\partial U_t} \frac{U_t}{M(U_t, V_t)}. \tag{39}$$

When the matching elasticity varies with tightness—as under a CES matching function — η_t^* is time-varying. By contrast, the baseline economy features a fixed Nash weight η, so the Hosios condition generally fails away from the steady state.

We therefore compute a *Hosios-efficient global path* by solving the same economy under the same aggregate shocks, but allowing the bargaining weight to adjust endogenously each period as $\eta_t = \eta_t^*(\theta_t)$. This benchmark can be interpreted as the allocation implemented by a competitive search environment (Moen, 1997; Wright et al., 2021), and it isolates the inefficiency induced by rigid surplus sharing in the presence of state-dependent tightness and endogenous separations.

Figure 9 compares the unemployment dynamics of the baseline model (dotted line) against the Hosios-efficient benchmark (solid line) under identical shock sequences. The difference is striking: the efficient economy exhibits significantly lower volatility. While the unconditional mean of unemployment is similar across both models ($\approx$ 4.5%), the volatility is markedly higher in the baseline economy (10.58%) compared to the efficient benchmark (8.71%).

This "efficiency gap" arises because the baseline economy fails to internalize the social cost of churn. During high-efficiency expansions, the fixed bargaining weight prevents wages from rising sufficiently to choke off excessive vacancy creation. This keeps the

value of a vacancy high, which, through the mechanism identified in Section 3, raises the reservation productivity threshold z_s too aggressively. The result is an inefficient spike in job separations.

Figure 9: The Efficiency Gap: Baseline vs. Hosios-Efficient Unemployment

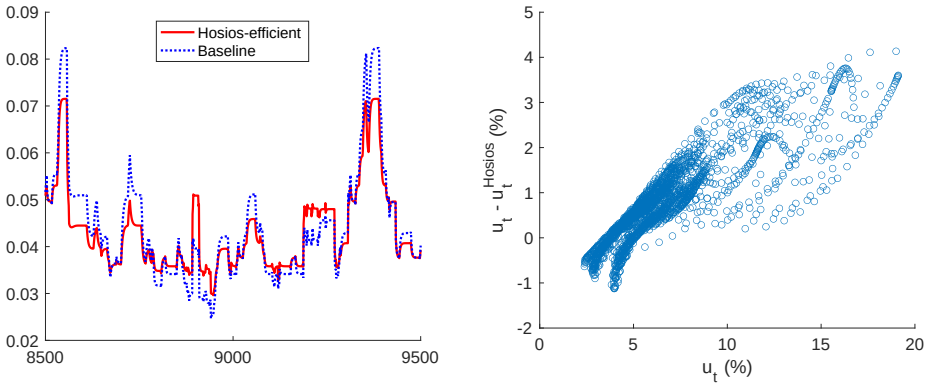

(a) Unemployment Time Series (b) Deviation from Efficiency

Table 7 quantifies these deviations across different states of the world. The inefficiency is state-dependent: the gap between the baseline and efficient outcomes widens significantly during periods of high matching efficiency, confirming that the "churning channel" is a primary source of welfare loss.

Table 7: Matching Efficiency and the Hosios Gap

	Average absolute distance from Hosios (%)			
	Baseline		Exogenous sep.	
	Unemp.	Vacancy	Unemp.	Vacancy
High ME	0.44	0.32	0.65	0.27
Low ME	0.34	0.21	0.74	0.42
Diff. $(High - Low)$	0.10	0.11	-0.09	-0.15

Notes: The table reports the average absolute deviation of the baseline economy from the Hosios-efficient benchmark across different matching efficiency (ME) regimes.

6.2 Taming the churn: Optimal policy analysis

Given that the baseline economy exhibits excessive volatility due to inefficient churn, we explore whether a simple fiscal instrument—a corporate tax (equivalent to a firing penalty)—can restore efficiency.

We focus our analysis on the two most recent recessions: the COVID-19 crisis (characterized by high matching efficiency) and the Great Recession (characterized by low matching efficiency). Using the generalized impulse response function (GIRF) method developed in Lee (2025), we simulate the economy's response to these shocks starting from their respective pre-crisis states.

Figure 10 displays the results. The solid blue line represents the baseline response, while the black line represents the Hosios-efficient path. During the COVID-19 recovery (Panel A), the baseline model predicts an excessive unemployment surge driven by the endogenous separation channel. The efficient planner would choose a path with significantly fewer separations.

Figure 10: State-Dependent Policy Effectiveness

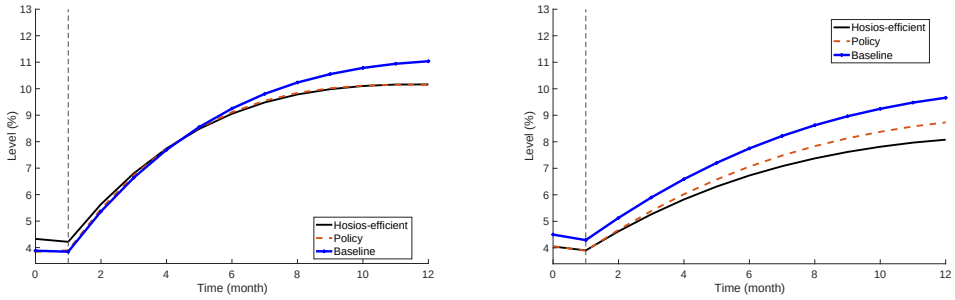

(a) COVID-19 Recession (High ME) (b) Great Recession (Low ME)

Can policy close this gap? We introduce a corporate tax τ (or equivalently, a firing penalty) and solve for the rate that minimizes the distance to the efficient path. We find that a *corporate tax of approximately 5%* is optimal.

As shown by the dashed lines in Figure 10, this policy effectively "tames the churn." By reducing the net value of the match, the tax lowers the sensitivity of the firm's outside option to matching efficiency shocks. Effectively, it acts as a circuit breaker on the separation elasticity $\frac{\partial \log s}{\partial \log m}$, preventing the massive outward shifts in the Beveridge curve that characterize the inefficient equilibrium. This finding suggests that

moderate firing costs, often criticized for reducing flexibility, may actually enhance welfare by dampening inefficient volatility in fluid labor markets.

6.3 The Risks of Ignoring Endogenous Separations

Finally, we use our framework to evaluate a standard stabilization policy: counter-cyclical unemployment benefits. We model a policy rule where benefits b increase by 5% when unemployment exceeds 6.5%, mirroring recent U.S. extensions.

Table 8 compares the impact of this policy in our baseline model versus a model with exogenous separations. The difference is substantial. In the exogenous separation model, the policy has a moderate impact. In our baseline model, however, the policy backfires: higher benefits raise the worker's outside option, which forces firms to raise the reservation productivity threshold even further. This triggers a secondary wave of endogenous separations, significantly increasing both the mean and volatility of unemployment.

This result serves as a cautionary tale: policy evaluations that ignore the endogenous separation margin—and specifically its interaction with matching efficiency—risk severely underestimating the volatility costs of interventions.

Table 8: The Impact of Counter-Cyclical Unemployment Benefits

	Unconditional		High ME		Low ME	
	$\mathbb{E}(u_t)$	$\sigma(u_t)$	$\mathbb{E}(u_t)$	$\sigma(u_t)$	$\mathbb{E}(u_t)$	$\sigma(u_t)$
baseline	4.591	10.829	5.566	11.904	4.066	13.936
baseline + counter-cyclical b	5.229	15.167	6.610	18.903	4.378	17.957
exo. sep.	6.843	11.343	5.624	13.470	8.129	13.844
exo. sep. + counter-cyclical b	7.507	13.866	6.090	17.161	8.983	16.900

7 Concluding remarks

This paper analyzes the Beveridge curve shifts through the lens of endogenous job destruction. We demonstrate that the standard intuition—that higher matching

efficiency unequivocally improves labor market outcomes—is incomplete. In high-efficiency regimes, a "churning channel" dominates, generating outward shifts in the Beveridge curve that models with exogenous separation fail to capture.

Our analysis reveals a distinct trade-off between matching efficiency and aggregate stability. We find that the decentralized equilibrium exhibits inefficiently high volatility due to excessive churning, which a modest corporate tax of 5% can optimally dampen. These results suggest a broader agenda for macro-labor research: moving beyond the study of frictional unemployment *levels* to understanding the welfare consequences of *turnover volatility* itself. Future work should explore how this endogenous instability interacts with inflation dynamics and the design of social insurance in markets characterized by rapid reallocation.

References

Barlevy, Gadi, R Jason Faberman, Bart Hobijn, and Ayşegül Şahin. 2024. "The Shifting Reasons for Beveridge Curve Shifts." *Journal of Economic Perspectives* 38 (2):83–106.

Barnichon, Regis. 2010. "Building a composite help-wanted index." *Economics Letters* 109 (3):175–178.

Barnichon, Régis and Adam Hale Shapiro. 2024. "Phillips Meets Beveridge." *Journal of Monetary Economics* :103660.

Crump, Richard K., Stefano Eusepi, Marc Giannoni, and Ayşegül Şahin. 2024. "The unemployment–inflation trade-off revisited: The Phillips curve in COVID times." *Journal of Monetary Economics* 145:103580. URL https://www.sciencedirect.com/science/article/pii/S0304393224000333. Inflation: Expectations & Dynamics October 14-15, 2022.

Den Haan, Wouter J, Garey Ramey, and Joel Watson. 2000. "Job destruction and propagation of shocks." *American Economic Review* 90 (3):482–498.

Elsby, Michael WL, Bart Hobijn, and Ayşegül Şahin. 2015. "On the importance of the participation margin for labor market fluctuations." *Journal of Monetary Economics* 72:64–82.

Fujita, Shigeru and Garey Ramey. 2012. "Exogenous versus endogenous separation." *American Economic Journal: Macroeconomics* 4 (4):68–93.

Hagedorn, Marcus and Iourii Manovskii. 2008. "The cyclical behavior of equilibrium unemployment and vacancies revisited." *American Economic Review* 98 (4):1692–1706.

Hodrick, Robert J and Edward C Prescott. 1997. "Postwar US business cycles: an empirical investigation." *Journal of Money, credit, and Banking* :1–16.

Jung, Philip and Keith Kuester. 2015. "Optimal labor-market policy in recessions." *American Economic Journal: Macroeconomics* 7 (2):124–156.

Lee, Hanbaek. 2025. "Global Nonlinear Solutions in Sequence Space and the Generalized Transition Function." *Working paper* .

Moen, Espen R. 1997. "Competitive search equilibrium." *Journal of political Economy* 105 (2):385–411.

Mortensen, Dale T and Christopher A Pissarides. 1994. "Job creation and job destruction in the theory of unemployment." *The Review of Economic Studies* 61 (3):397–415.

Petrongolo, Barbara and Christopher A. Pissarides. 2001. "Looking into the Black Box: A Survey of the Matching Function." *Journal of Economic Literature* 39 (2):390–431.

Petrosky-Nadeau, Nicolas and Lu Zhang. 2017. "Solving the Diamond–Mortensen–Pissarides model accurately." *Quantitative Economics* 8 (2):611–650.

———. 2021. "Unemployment crises." *Journal of Monetary Economics* 117:335–353. URL https://www.sciencedirect.com/science/article/pii/S0304393220300064.

Pissarides, Christopher A. 2000. *Equilibrium unemployment theory*. MIT press.

Rotemberg, Julio J. 1999. "A heuristic method for extracting smooth trends from economic time series."

Sedláček, Petr. 2014. "Match efficiency and firms' hiring standards." *Journal of Monetary Economics* 62:123–133.

Shimer, Robert. 2005. "The cyclical behavior of equilibrium unemployment and vacancies." *American Economic Review* 95 (1):25–49.

Wright, Randall, Philipp Kircher, Benoît Julien, and Veronica Guerrieri. 2021. "Directed search and competitive search equilibrium: A guided tour." *Journal of Economic Literature* 59 (1):90–148.

Yashiv, Eran. 2007. "Labor search and matching in macroeconomics." *European Economic Review* 51 (8):1859–1895.